Available online at www.sciencedirect.com
SCIENCE DIRECT®
International Journal of Thermal Sciences 42 (2003) 561–569
International Journal of Thermal Sciences
www.elsevier.com/locate/ijts

Convective heat transfer from a billet due to an oblique impinging circular jet within the spray forming process

Olaf Meyer, Alexander Schneider, Volker Uhlenwinkel *, Udo Fritsching

Universität Bremen, Special Research Centre "Spray Forming", Badgasteiner Str. 3, 28359 Bremen, Germany

Received 20 February 2002; accepted 26 July 2002

Abstract

An experimental investigation was performed to study the heat transfer process from the surface of a billet due to an oblique impinging circular gas jet. The gas stream was generated by a circular array of 24 single jets within an atomizer nozzle. The application of this heat transfer condition can be found in the spray forming process during the cooling of the sprayed billet. At several positions on the billet surface the local heat transfer coefficients were measured. The measurement technique was based on the cooling of a surface mounted sensor having a sufficiently small Biot number. A comparison between published data and a test case had been carried out successfully. The distance between the atomizer and the billet, the gas mass flow rate, and the rotation angle of the billet were varied. Velocity measurements were executed to characterise the gas flow in the confined jet in the absence of the billet, while numerical flow field simulations were used to calculate the flow around the billet. The heat transfer coefficient distribution showed a significant peak at the stagnation point and decreased with increasing atomizer to billet distance and also with decreasing gas mass flow. The heat transfer coefficients averaged over the circumference of the billet were correlated empirically.

Résumé

Une étude expérimentale est effectuée pour étudier le transfert de chaleur, à la surface d'une billette, crée par un courant circulaire gazeux d'impact oblique. Le courant gazeux est généré par un anneau de 24 jets simples. Cette condition de transfert de chaleur se produit dans le procédé de mise en forme par atomisation lors du refroidissement de la billette pulvérisée. Les coefficients de transferts de chaleur locaux ont été mesurés à différentes positions sur la billette. La technique de mesure est basée sur le refroidissement d'un palpeur ayant un nombre de Biot suffisamment petit. Une comparaison entre les données publiées et le cas testé a été effectuée avec succès. La distance entre l'atomiseur et la billette, le flux massique de gaz et l'angle de rotation de la billette étaient les paramètres qui variaient. Des mesures de vitesses ont été entreprises pour caractériser le flux de gaz sans billette alors que des simulations numériques furent utilisées pour calculer le flux avec billette. Le coefficient de transfert de chaleur est maximal au point d'impact et diminue avec l'augmentation de la distance atomiseur/billette mais diminue aussi avec la réduction du flux massique de gaz. Les coefficients de transfert de chaleur moyennés sur la circonférence sont mis en corrélation d'une manière empirique.

Keywords: Spray forming; Convective heat transfer; Jet impingement; Measurement technique; Heat transfer coefficient

Mots-clés : Mise en forme par atomisation ; Transfert de chaleur par convection ; Impact par jet ; Technique de mesure ; Coefficient de transfert de chaleur

* Corresponding author.
E-mail address: uhl@iwt.uni-bremen.de (V. Uhlenwinkel).

1290-0729/03/$ – see front matter
doi:10.1016/S1290-0729(03)00022-X

Nomenclature

A	surface	m^2	
a	thermal diffusion coefficient	$m^2 \cdot s^{-1}$	
Bi	Biot number		
c	speed of sound	$m \cdot s^{-1}$	
c_p	specific heat	$J \cdot kg^{-1} \cdot K^{-1}$	
D	nozzle diameter	m	
d	diameter	m	
H	total height of the billet	m	
h	distance from the billet top	m	
i	number		
L	length of sensor	m	
l	distance of billet centre	m	
M	measurement point		
$\dot{M}_G$	gas mass flow rate	$kg \cdot s^{-1}$	
n	number		
Nu	Nusselt number		
Pr	Prandtl number		
p	pressure	MPa	
p_z	absolute nozzle pressure	MPa	
p_U	absolute ambient pressure	MPa	
p_0	dimensionless gas pressure		
u	axial gas velocity	$m \cdot s^{-1}$	
u_m	velocity at the centre of the gas stream	$m \cdot s^{-1}$	
R	distance from impinging point	m	
Re	Reynolds number		
r	radius	m	
$r_{0.5}$	half radius	m	
r^*	dimensionless radius		
T	temperature	°C, K	
Tu	turbulence intensity	%	
T_∞	temperature of the impinging gas	°C, K	
t	time	s	
V	volume	m^3	
z	distance between nozzle and billet	m	
z^*	dimensionless distance (nozzle-plate)		

Greek symbols

α	heat transfer coefficient	$W \cdot m^{-2} \cdot K^{-1}$
$\bar{\alpha}$	average heat transfer coefficient	$W \cdot m^{-2} \cdot K^{-1}$
$\bar{\alpha}_{top}$	average heat transfer coefficient at the billet top	$W \cdot m^{-2} \cdot K^{-1}$
$\bar{\alpha}_{jacket}$	average heat transfer coefficient at the billet jacket	$W \cdot m^{-2} \cdot K^{-1}$
ρ	density	$kg \cdot m^{-3}$
ε	eccentricity	m
λ	thermal conductivity	$W \cdot m^{-1} \cdot K^{-1}$
φ	rotation angle of the billet	°
ν	kinematic viscosity	$kg \cdot m^{-1} \cdot s^{-1}$
σ	standard deviation	

1. Introduction

During the production of spray formed[1] billets [1–3] the cooling rate is an important parameter because it mainly affects the material properties of the as-sprayed and the final product. Grain growth, carbide size, segregation, and residual stresses are some of the material properties that the cooling rate affects. The heat transfer due to convection is one of the most important boundary conditions for the thermal history of a spray formed billet [4]. Therefore, local heat transfer coefficients must be chosen carefully to get proper results of temperature history and grain size from numerical simulations.

The heat transfer due to jet impingement has been the subject of many previous investigations. Most of the investigations in this field of research are concerned with orthogonal jets impinging onto a plane surface. For example, a survey of different contributions about these geometrical conditions was published by Jambunatan et al. [5]. Investigations of jets impinging on a curved surface have also been frequently encountered in different papers. Some authors examined slot jet impingement on a curved surface [6–9]. This however is a two-dimensional situation unlike the flow situation within a circular jet. The impingement of a circular jet on a cylindrical body was studied, e.g., by Sparrow et al. [10] and Tawfek [11]. The cylinder in the Sparrow and Tawfek's cases were in crossflow. Both authors determined the peak value of the heat transfer coefficient at the impingement point. Furthermore, their results indicated, that with decreasing distance between nozzle and cylinder and increasing nozzle diameter the heat transfer coefficient increases.

The geometric conditions of these previous investigations do not meet those of the spray forming application. In spray forming, a gas stream generated by a free fall atomizer nozzle impinges oblique onto the top and the jacket of a billet. Fig. 1 shows both, the spray formed billet (right) in the spray chamber, and the billet dummy (left) used in this investigation to carry out measurements to determine local heat transfer coefficients. The gas flow generated by the nozzle was characterized by means of velocity and turbulence measurements. To achieve realistic boundary conditions the billet dummy was placed inside a spray chamber. A robust measurement technique was chosen to overcome problems with particles and dust in the spray chamber which may destroy fragile sensors like hot wire probes. The gas flow rate and the distance between billet and atomizer were the varied parameters under investigation.

[1] Spray forming is a relatively new process to produce metal preforms with improved material properties due to the rapid cooling of the material within the spray and the subsequent cooling period.

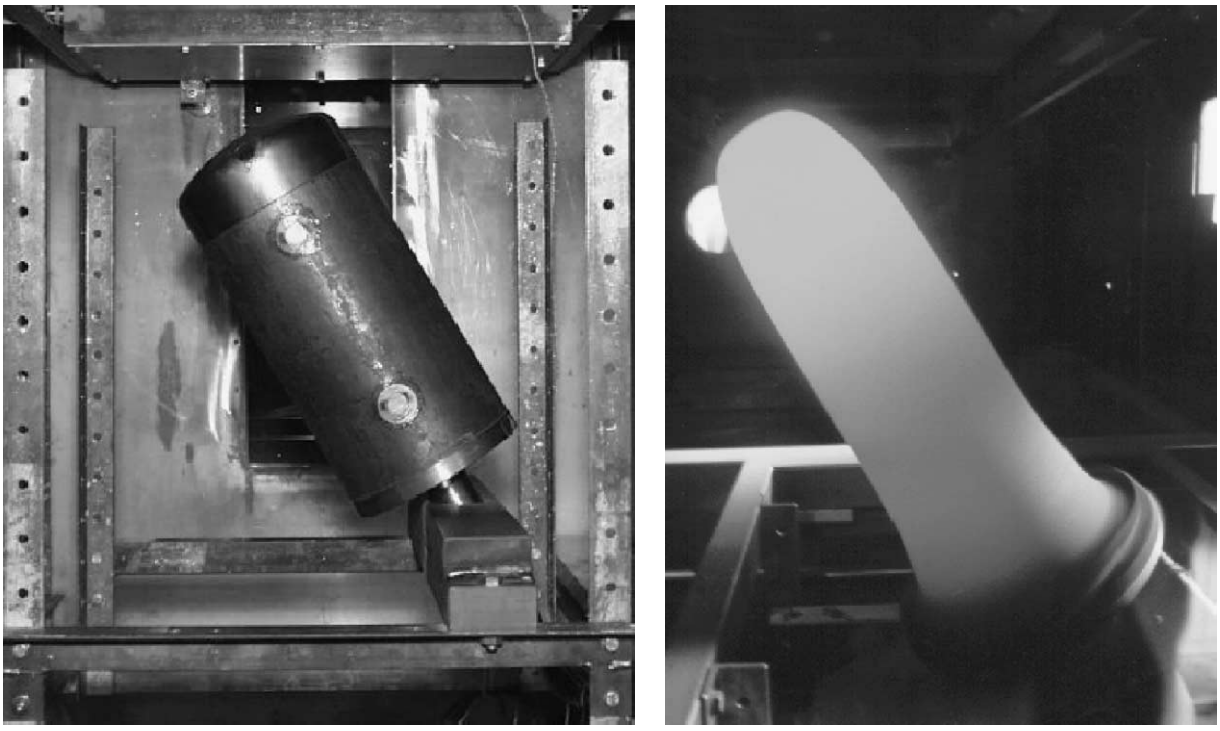

Fig. 1. Billet dummy and spray formed billet.

2. Measurement technique and test section

First a suitable method was created for measurement of the heat transfer coefficient under the aggressive general conditions. An important criterion was the sensors robustness against mechanical strain. The measurements were carried out in a original spray chamber for spray forming applications in which a significant remaining particle concentration was observed from preceding spray forming experiments. These particles were a threat to the measurement device. The measurement technique was based on the cooling of a sensor having a sufficiently small Biot number ($Bi \geqslant 0$). For such a sensor the heat transfer on the surface is the limiting factor for the heat transport from the body to the ambient gas [12]. The temperature gradient within the body can be neglected if the Biot number is small enough. In this case a simple energy balance for the sensor can be written as [12],

$$c_p \rho V \frac{\mathrm{d}T}{\mathrm{d}t} = -A\alpha(T - T_\infty) \tag{1}$$

were c_p is the heat capacity of the sensor, ρ the density, V the sensor volume, T_∞ the temperature of the impinging gas and A the surface of the sensor in contact with the gas. With this equation the heat transfer coefficient α on the sensor surface A can be determined from the time dependent temperature change ($\mathrm{d}T/\mathrm{d}t$). The sensor was designed as a cylindrical body surrounded by an insulation to make sure that heat flow only occurs at the sensor surface A (Fig. 2). Hence from Eq. (1) and with the chosen geometry this leads

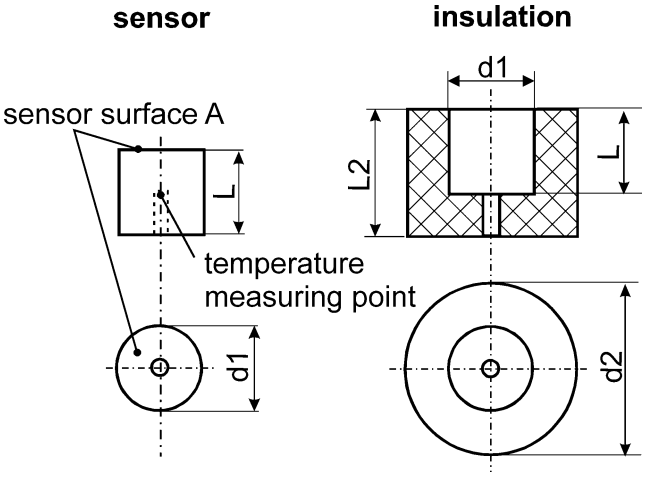

Fig. 2. Test body for the measurement of the heat transfer coefficient and insulating body.

to the relationship

$$\alpha = -\frac{\rho L c_p}{t_m} \ln\left(\frac{T_{\mathrm{end}} - T_\infty}{T_{\mathrm{start}} - T_\infty}\right) \tag{2}$$

for the heat transfer coefficient $\alpha \cdot T_{\mathrm{start}}$ is the temperature of the sensor at the beginning of the measurement, T_{end} the temperature after the measurement time t_m and L the length of the sensor. The insulation has a very low thermal conductivity of $\lambda < 0.1\ \mathrm{W{\cdot}m^{-1}{\cdot}K^{-1}}$ to minimise heat losses. For measurement of the temperature a thermocouple was placed in the middle of the sensor. Several sensors at different posi-

tions on the billet surface were used simultaneously for the measurement of local heat transfer coefficient distributions.

In order to test the accuracy of the measurement technique some preliminary experiments have been carried out for a single circular jet impinging orthogonally onto a planar surface. Therefore the insulated sensor was fitted into a plate. The measured heat transfer coefficients are compared with already published data. A single cylindrical nozzle was employed for the generation of the air jet. The nozzle exit velocity and the distance H between the nozzle and the plate could be varied. A uniform velocity profile and low turbulence levels at the nozzle exit are guaranteed. The sensor has been positioned under the point of impingement and was heated to temperatures between 200 °C and 240 °C before the experiment started. During the experiment the transient temperatures of the sensor and the air jet were measured by thermocouples. The measured heat transfer coefficients are compared to a relation from [13]

$$Nu = \frac{1 - 1.1/r^*}{r^* + 0.1 \cdot (z^* - 6)} \cdot F(Re) \cdot Pr^{0.4} \tag{3}$$

with

$$F(Re) = 2 \cdot \left[Re \cdot \left(1 + 0.005 \cdot Re^{0.55}\right)\right]^{0.5} \tag{4}$$

and

$$r^* = \frac{R}{D}, \qquad z^* = \frac{z}{D} \tag{5}$$

for an impinging round jet onto a plane surface. This empirical correlation is valid for

$$2.5 \leqslant r^* \leqslant 7.5, \quad 2.0 \leqslant z^* \leqslant 12.0 \quad \text{and}$$
$$2000 \leqslant Re \leqslant 400\,000 \tag{6}$$

with

$$Nu = \frac{\alpha \cdot D}{\lambda_{\text{fluid}}}, \qquad Bi = \frac{\alpha \cdot D}{\lambda_{\text{solid}}}$$
$$Pr = \frac{\nu}{a} \quad \text{and} \quad Re = \frac{u_0 \cdot D}{\nu} \tag{7}$$

in which for the material properties of the fluid an averaged mean temperature between the sensor and the nozzle exit ($\overline{T} = (T_{\text{nozzle}} + T_{\text{sensor}})/2$) is used. The Nusselt number and the heat transfer coefficient α are mean values on the heated surface with radius R. Important material properties of the fluid are the thermal conductivity λ_{fluid}, the kinematic viscosity ν, and the thermal diffusion coefficient a. The distance R is the radial distance from the impingement point on the plane surface, u_0 the gas velocity at the nozzle exit, and D the diameter of the nozzle exit ($D = 3.81$ mm). However in this case the radial distance R corresponds to the radius of the sensor ($R = 10$ mm). In order to select the most suitable sensor, different geometrical sensor dimensions and materials have been tested. Materials with a high thermal conductivity are preferred in order to guarantee a small Biot number. The measured heat transfer coefficients can be computed from Eq. (2). In each case they are averaged for an experimental time t_m of 60 s. The best comparison between the measured data and Eq. (2) were achieved with a copper sensor ($\rho = 8930$ kg·m^{-3}, $c_p = 382$ J·kg^{-1}·K^{-1}, $\lambda_{\text{solid}} = 364$ W·m^{-1}·K^{-1}). The diameter d_1 and the length L of this sensor were 20 mm each ($d_1 = L = 20$ mm). During the investigations the ratio between the nozzle diameter D and the distance H were $H/D = 4$ and $H/D = 6$ respectively and the nozzle Reynolds number ranged from 4000 to 40 000. The measured heat transfer coefficients for the copper sensor are plotted in Fig. 3 versus the Reynolds number. In general, the measured data reflects the tendency as predicted by Eq. (3). The heat transfer coefficient increases with increasing Reynolds number as expected and decreases with increasing distance between nozzle and impingement point. However, there is a difference between the measured data and the used correlation. But a review of different heat transfer data also shows a considerable scatter of experimental results [5]. One reason for this difference is the limited reproducibility of the gas jet parameters (turbulence, velocity profile). These boundary conditions are often not measured or reported properly in the literature. Furthermore the increase of the Biot number and heat transfer coefficient as well must be taken into consideration, because Eq. (1) is valid only for a low Biot number. On the other hand, in this study the Biot number was always below 0.07, which is low enough for the assumed simplification. The reproducibility of the heat transfer coefficient measurements at the impingement point was good (maximum standard deviation of 5.1 W·m^{-2}·K^{-1}).

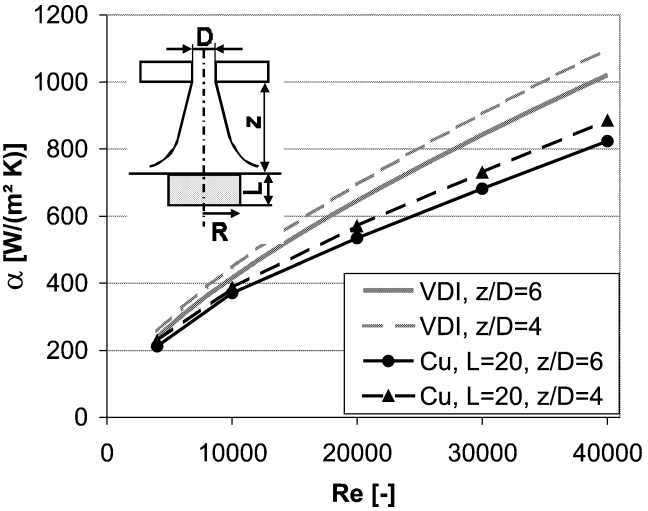

Fig. 3. Comparison between measured, mean heat transfer coefficient α at the stagnation point within an impinging jet and literature [13].

3. Experimental set up and procedure

For the measurement of local heat transfer coefficients seven measurement positions on the surface of the billet dummy were used. The copper cylinder which was selected

during the test section is used as the sensor ($L = d_1 = 20$ mm). Fig. 4 shows a cross section of the billet dummy and the different measurement positions. The dimensions of the dummy were taken from averaged real billet shapes which had been spray formed in our own plants (Fig. 1). The experiments were carried out in a rectangular spray forming chamber. In Fig. 5 the experimental set-up within the spray chamber and the description of the billet dummy orientation within the gas stream are shown. The billet was aligned with a setting angle of 30° from the axis of the gas stream. This setting angle was proven for the spray forming of billets and remained constant in all experiments. Although the billet dummy can be rotated around its axis in order to achieve different angular positions φ of the sensors. For an eccentricity $\varepsilon = 84$ mm (distance between billet axis and impinging point) and a rotation angle $\varphi = 0°$ the axis of the gas stream impinged exactly on the middle of the measurement point $M3$ (Fig. 4). During the experiments the distance z between the atomizer and the stagnation point was varied in the range $z = 400$–500 mm. Thermocouples were placed within the sensors, one at the inner wall of the billet and one below the atomizer within the gas stream. The measured temperature signals were recorded. Nitrogen was used to generate the gas stream because most of the spray forming experiments were carried out with nitrogen. The entire billet dummy and the sensors were heated to a constant temperature of 110–150 °C before the gas stream was turned on. This allowed the evolution of a continuous thermal boundary layer over the entire surface of the billet. The thermal history of each sensor was recorded over a time period of 60 s. From the measured data the heat transfer coefficients were determined by Eq. (2) and averaged over the measured time period. The atomizer consists of 24 round individual nozzles (diameter 4 mm) in a circular arrangement. It was characterised by a circular diameter of 40 mm and an exit angle of 10° [14]. The gas flow was varied between 0.2 and 0.29 kg·s^{-1}. Velocity measurements were carried out (with a hot wire anemometer) to characterise the flow field of the atomizer. With consideration of the measured velocities and turbulence levels within the gas jet the gas flow around the billet was calculated by a simulation program and are discussed with regard to the measured heat transfer coefficients.

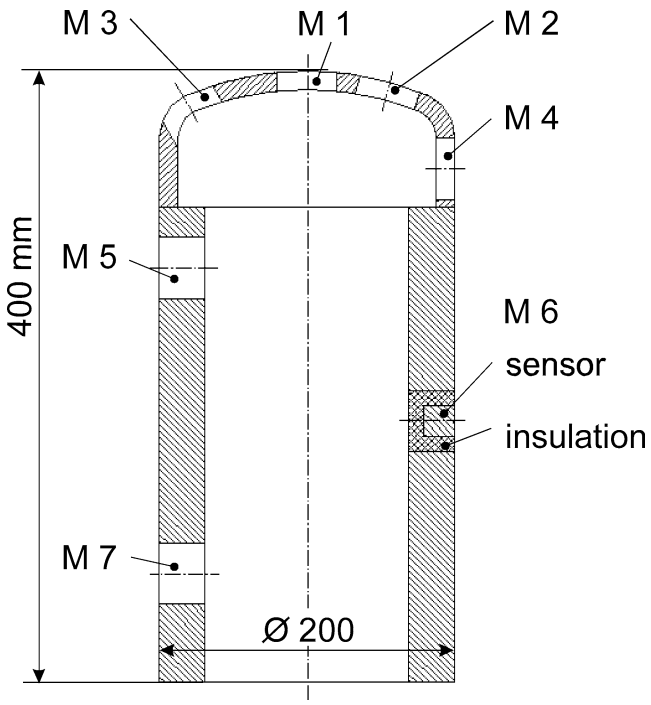

Fig. 4. Outline of the billet dummy and measurement positions ($M1$–$M7$).

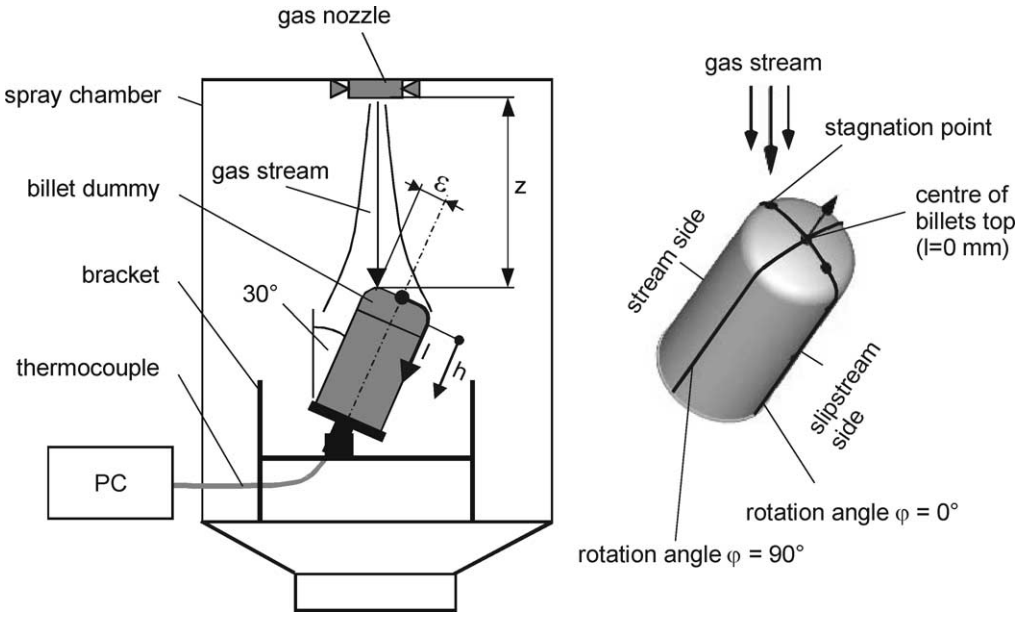

Fig. 5. Schematic diagram of the measurement arrangement within the spray chamber and description of the billet dummy orientation within gas jet.

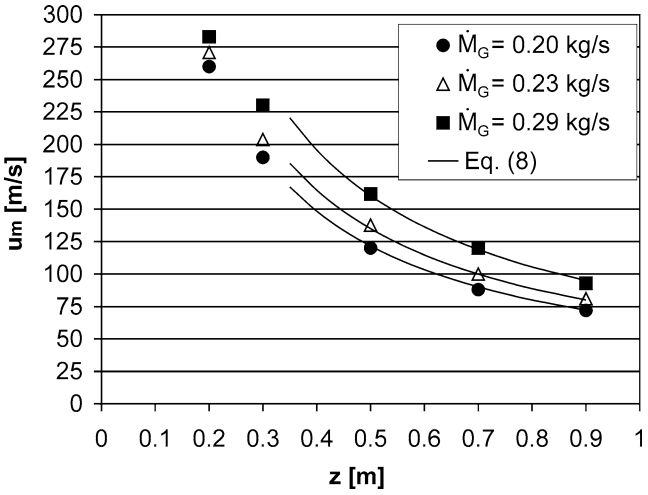

Fig. 6. Maximum gas velocity u_m of the jet stream in dependence of the nozzle distance z and the gas mass flow $\dot{M}_G$.

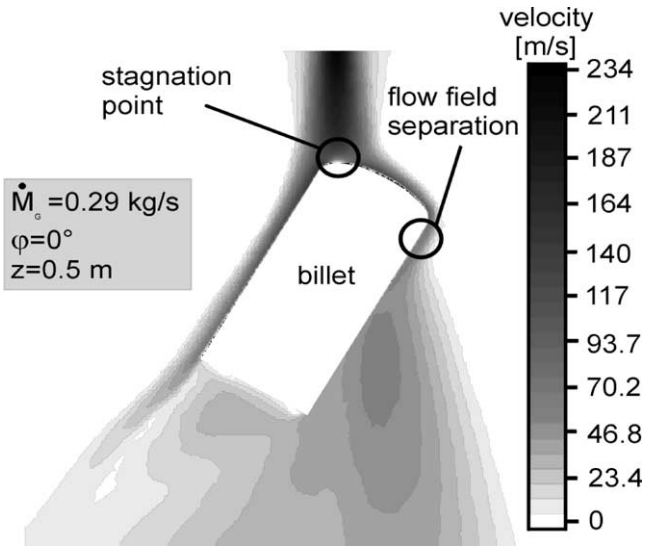

Fig. 7. Simulated velocity magnitude around the billet within a cross section of the 3-D simulation with $\dot{M}_G = 0.29$ kg·s^{-1}, $z = 0.5$ m and $\varphi = 0°$.

4. Results and discussion

4.1. Velocity and turbulence intensity of the gas flow field

The local heat transfer coefficient α at a round billet in a gas stream depend basically on the local gas velocities u and the turbulence intensity Tu. In order to study their effect on local heat transfer coefficients both were measured by a one-dimensional hot wire CTA probe (Constant Temperature Anemometer), while the atomizer gas mass flow $\dot{M}_G$, the axial distance z, and the radial distance r were varied in the undisturbed gas stream (without billet). Fig. 6 shows the axial velocity u_m at the centre of the gas flow ($r = 0$ m) in dependence of the distance z for the gas mass flows $\dot{M}_G = 0.2$, 0.23, and 0.29 kg·s^{-1}.

With increasing distance z to the atomizer the velocity u_m decreases. The decrease of the velocity u_m is correlated using an equation suggested by Koria [15] for underexpanded free jets:

$$u_m = 2.4 \cdot c \cdot p_0^{0.775} \cdot \left(\frac{D}{z}\right)^{0.89} \quad \text{and} \tag{8}$$

$$p_0 = \left(\frac{p_Z}{p_U}\right) \tag{9}$$

In Eq. (8) c is the velocity of sound $c = 343$ m·s^{-1} (for nitrogen at a temperature of app. 10 °C at the nozzle exit), p_0 the dimensionless nozzle pressure as the ratio of the absolute nozzle pressure p_Z to the ambient pressure p_U, and D the diameter of the nozzle (here $D = 0.0196$ m). For a pressure ratio $p_0 \geqslant 1.89$ for underexpanded gas (nitrogen) jets, a linear relation between p_0 and gas mass flow $\dot{M}_G$ can be found. The following empirical correlation was determined:

$$\dot{M}_G\ [\text{kg·s}^{-1}] = 0.0605 \cdot p_0[-] - 0.0158 \tag{10}$$

The axial velocities at different radial positions show a typical free jet distribution (not shown here) and lead to the following linear relation for the half velocity radius $r_{0.5}$ in dependence of the distance z:

$$r_{0.5} = 0.088 \cdot z \quad \text{for } z = 0.3{-}0.8 \text{ m} \tag{11}$$

In the centre of this gas jet (-10 mm $< r <$ 10 mm) at distances $z > 0.3$ m the turbulence intensity was almost constant with a turbulence intensity value Tu app. 23%. With increasing radius the turbulence intensity increased up to $Tu = 50\%$ for $r > 50$ mm. A change in the gas mass flow rate $\dot{M}_G$ from 0.2 to 0.29 kg·s^{-1} did not lead to any significant changes in the turbulence intensity.

Fig. 7 shows the computed gas velocity magnitude around the billet dummy. The three-dimensional simulation was carried out with FLUENT 4.0. The velocity field (absolute value) is presented for a cross section of the billet, an eccentricity of $\varepsilon = 84$ mm, and a gas mass flow of $\dot{M}_G = 0.29$ kg·s^{-1}. For modelling of the gas stream the measured boundary conditions, velocity u, and turbulence intensity Tu, were used at the inlet. From the low velocity above the measurement point, $M3$, the point of impingement can be identified (left side of the billet top). Furthermore the simulated gas velocity on the left side of the billet is relatively high. Due to this a relatively high heat transfer coefficient can be expected in this area. In contrast to this a flow field separation below the edge of the billet top and a lower absolute velocity values can be observed on the right side of the billet. Due to the flow field separation at the edge of the billet top a distinct change of the heat transfer coefficient distribution in flow direction can be expected.

4.2. Reproducibility of the measuring system

The reproducibility of the measurement system was checked by three individual measurements at identical flow conditions. The billet dummy was positioned in the gas stream ($z = 0.4$ m, $\dot{M}_G = 0.2$ kg·s^{-1}) in a way, that in the

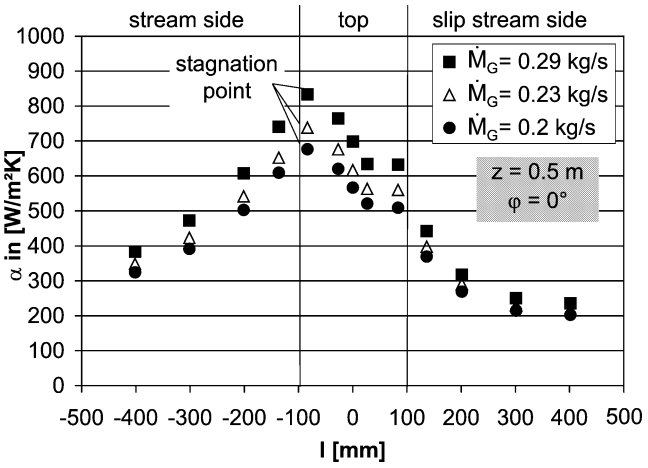

Fig. 8. Measured heat transfer coefficients α at different distances to the billet centre l in dependence of the gas mass flow $\dot{M}_G$ for $z = 0.5$ m and $\varphi = 0°$.

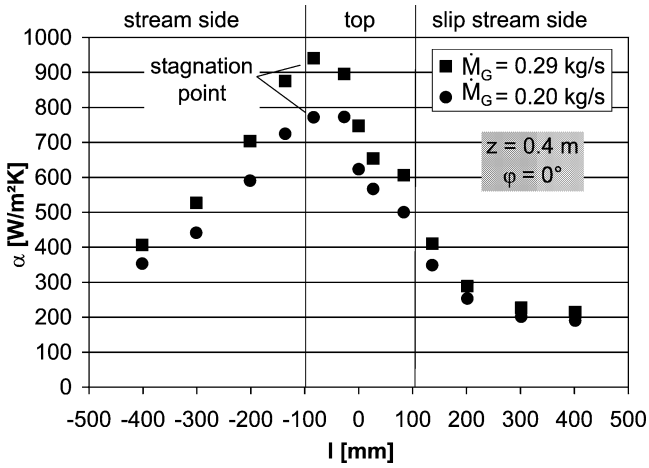

Fig. 9. Heat transfer coefficients α at a distance $z = 0.4$ m and $\varphi = 0°$.

position $\varphi = 0°$ the stagnation point was similar to the point $M3$ as explained earlier. The highest standard deviation σ was calculated for point $M3$ at the stagnation point with an average heat transfer coefficient of $\alpha = 756$ W·m^{-2}·K^{-1} and $\sigma = 14$ W·m^{-2}·K^{-1}. This is equivalent to a relative standard deviation of 2% which also holds for the other measurement points.

4.3. Local heat transfer coefficients α

Local heat transfer coefficients α versus the location on the billet surface for different gas mass flows $\dot{M}_G = 0.2$, 0.23 and 0.29 kg·s^{-1} are plotted in Fig. 8. The values are valid for a distance $z = 0.5$ m between atomizer and billet and an angle $\varphi = 0°$. L is the distance from the centre of the billet following the surface.

An increase of the gas mass flow rate $\dot{M}_G$ of 0.2, 0.23 and 0.29 kg·s^{-1} leads to an increase of the local heat transfer coefficient α at the stagnation point of 680, 730, and 830 W·m^{-2}·K^{-1}, respectively. At the stagnation point the local heat transfer coefficient reached its maximum and decreased exponentially at the top surface of the billet ($l = 100$ mm). A similar behaviour was observed in both the stream and slip stream side of the billet (see also Fig. 5). It can be stated that the convective heat transfer is approximately twice as high on the stream side compared to the slip stream side. At the edge of the billet top at $l = 100$ mm the exponential drop of the heat transfer coefficient is interrupted. This effect could be explained by a flow field separation and a matching vortex formation at the billet edge, as expected from the simulation. The rising turbulence intensity through vortex formation leads to an increased convective heat transfer at the billet edge.

Similar to the results shown previously, the local heat transfer coefficients for a smaller distance of $z = 0.4$ m for $\dot{M}_G = 0.2$ and 0.29 kg·s^{-1} are represented in Fig. 9. The maximum heat transfer coefficient at the stagnation

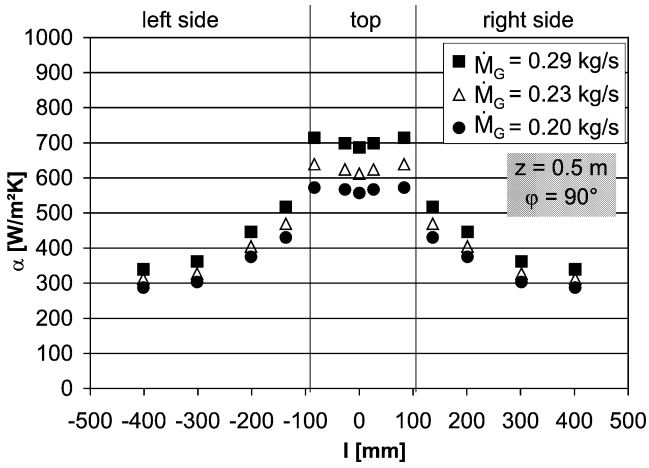

Fig. 10. Heat transfer coefficients α at a distance $z = 0.5$ m and $\varphi = 90°$.

point increased by 100 W·m^{-2}·K^{-1} due to the reduction of the distance z, which can be explained by the increase of the local velocity u. Starting from the stagnation point the heat transfer coefficient distribution to both sides is analogous to $z = 0.5$ m. Furthermore between $l = 50$ mm and 100 mm at the billet top a clear bend in the graph can be recognized, which confirms the presumption of a vortex formation through a flow field separation. Additionally it can be seen that the local heat transfer coefficients at the bottom of the billet for $l = \pm 400$ mm is mainly not affected by the reduction of the distance.

In Fig. 10 the local heat transfer coefficients are shown for a distance of $z = 0.5$ m, $\dot{M}_G = 0.2$, 0.23 and 0.29 kg·s^{-1} in the position $\varphi = 90°$. The measured local heat transfer coefficients are axi-symmetrical around the billet centre ($l =$ 0 mm). From the centre towards the edge on the billet top, the local heat transfer coefficient is nearly constant. At the billet sides the heat transfer declines exponentially for larger distances of l.

4.4. Correlation for averaged heat transfer coefficients α

In the spray forming process the billet rotates at a low rotation speed compared to the velocities of the gas stream. During one revolution a surface segment of the billet passes the complete rotation angle φ. The heat transfer problem can be simplified using average heat transfer coefficients during one revolution. First, a correlation for the averaged heat transfer coefficient at constant distances l on the billet top was developed. To calculate the averaged value $\bar{\alpha}$, the local heat transfer coefficients at a constant distance l from the centre of the billet were taken:

$$\bar{\alpha}(l) = \frac{\sum_{i=1}^{n} \alpha_i}{n} \tag{12}$$

where i stands for different rotation angles φ. In this case $\Delta\varphi = 90°$ and $\varphi_1 = 0°$. The result at the top of the billet was a constant averaged heat transfer coefficient. At the centre ($l = 0$ mm) the average value is constant by definition, because the location is not changing with rotation angle. And the local values just oscillate around the average value at the other locations ($l \neq 0$ mm) at the billet top. In the end one only needs to measure at a single position ($l = 0$ mm) to know the averaged value at all locations on the top. This means that the average heat transfer coefficient at the billet top only depends on the distance z and the gas mass flow of the nozzle $\dot{M}_G$.

In principle, the convective heat transfer of a body in a gas stream depends on the gas velocity field and its turbulence intensity, because these influence the velocity and thermal boundary layer at the body. The results of the hot wire measurements in the gas stream show that the turbulence intensity Tu does not change significantly for the chosen parameter range. This means that the turbulence intensity does not have to be considered separately and the maximum velocity u_m in the centre of the jet and the half radius $r_{0.5}$ describe the flow field of the jet stream the best, which can be easily calculated from Eqs. (8), (10) and (11) for the gas mass flow $\dot{M}_G$ and distance z. In Fig. 11 the average heat transfer coefficient $\bar{\alpha}$ at the billet top (100 mm $< l <$ −100 mm) is plotted versus $(u_m \cdot \sqrt{r_{0.5}})$. There seems to be a linear regression between these values, which can be expressed by the following empirical correlation:

$$\bar{\alpha}_{\text{top}}[\text{W}\cdot\text{m}^{-2}\cdot\text{K}^{-1}] = 16.2 \cdot u_m[\text{m}\cdot\text{s}^{-1}] \cdot \sqrt{r_{0.5}[\text{m}]} + 165 \tag{13}$$

This equation is limited to the boundary conditions and parameter ranges of this study: $z = 0.4$ to 0.5 m, $\dot{M}_G = 0.2$ to 0.29 kg·s^{-1}, $Tu \sim 23\%$, nitrogen and a 30° billet angle. The average heat transfer coefficient using the same averaging procedure, see Eq. (12), at the side of the billet for one revolution was calculated as well. The results were correlated with the dimensionless height h/H ($H = 400$ mm) using an exponential function, where $h/H = 0$ is the billet top, and $h/H = 1$ is the bottom of the billet. The best fit was obtained for the following correlation:

$$\bar{\alpha}_{\text{jacket}}\left(\frac{h}{H}\right) = \bar{\alpha}_{\text{top}} \cdot e^{[0.85\cdot(h/H)^2 - 1.65\cdot(h/H)]} \tag{14}$$

A comparison between averaged heat transfer coefficients and Eq. (14) can be seen in Fig. 12. Averaged heat transfer coefficients correlate very well with Eq. (14). In principle, both an increase of gas mass flow rate $\dot{M}_G$ and the reduction of the distance z leads to increasing axial velocities of the gas stream, and finally to increasing convective heat transfer. Identical limits for Eqs. (13) and (14) have to be noticed as validation ranges. Further measurements are necessary to find correlations for the heat transfer which can be used in a more common way (like a Nusselt–Reynolds correlation).

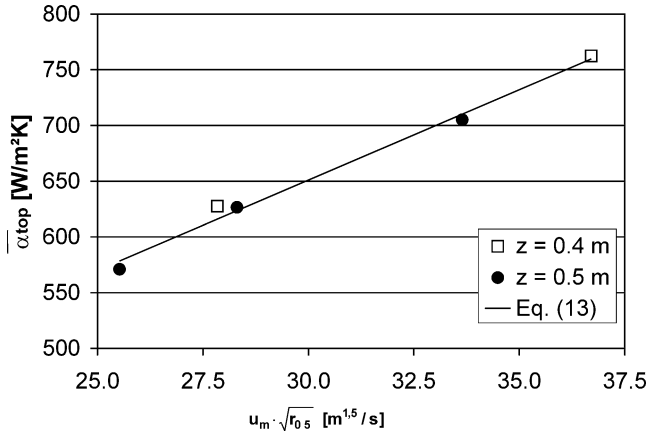

Fig. 11. Correlation of the average heat transfer coefficient $\bar{\alpha}_{\text{top}}$ at the top of the billet.

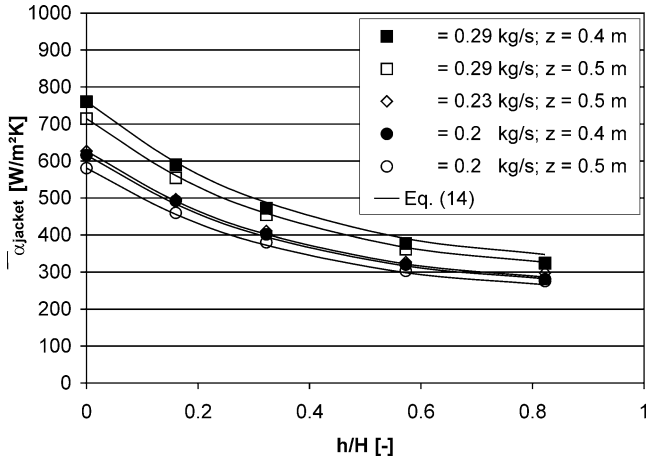

Fig. 12. Average heat transfer coefficient $\bar{\alpha}_{\text{jacket}}$ at the billet jacket.

5. Summary and conclusions

Results of the heat transfer on the surface of a billet due to an oblique impinging circular gas stream are reported. The circular stream has been generated by a round array of 24

single jets within an atomizer nozzle. This special geometrical arrangement occurs in the spray forming process during the cooling of the spray formed billets. For detection of local heat transfer coefficients a suitable measurement technique was selected, which is based on cooling of a cylindrical sensor having a sufficiently small Biot number. The accuracy of this sensor was examined using a set-up with a single jet impinging normal to a plate. The heat transfer coefficients from the tests are in agreement with published data. Furthermore the reproducibility of the measured heat transfer coefficients was good (relative standard deviation better then 2%). For different positions on the billet surface local heat transfer coefficients have been measured. The gas mass flow rate ($\dot{M}_G = 0.2, 0.23, 0.29\ \mathrm{kg{\cdot}s^{-1}}$) and the distance between nozzle system and billet dummy ($z = 0.4, 0.5\ \mathrm{m}$) have been changed. For the characterization of the gas stream the velocities and the turbulence intensity at different positions were measured. Also, a simulation of the gas flow around the billet was carried out and discussed with the measured heat transfer coefficients. On the slipstream side of the billet a flow field separation can be observed within the computed velocity field and also a distinct change of the measured heat transfer coefficients within the same zone has been found. The maximum heat transfer coefficient has been measured at the stagnation point and ranges from 650 to 950 $\mathrm{W{\cdot}m^{-2}{\cdot}K^{-1}}$ for the used parameters. The measured local heat transfer coefficients were averaged over the circumference of the billet. These averaged heat transfer coefficients were correlated empirically. The averaged heat transfer coefficient at the billet top does not depend on the radial distance from the billet centre. An empirical equation is given to describe the averaged heat transfer coefficient at the billet top depending on the gas velocity and the half radius. The decrease of the averaged heat transfer coefficient on the billet jacket can be described by an exponential function.

Acknowledgements

The authors gratefully acknowledge the support of the Deutsche Forschungsgemeinschaft (DFG), Collaborative Research Centre 372 of the University Bremen, Germany.

References

[1] E.J. Lavernia, Y. Wu, Spray Atomization and Deposition, Wiley, Chichester, 1996.

[2] K. Hummert, PM-Hochleistungsaluminium im industriellen Maßstab, in: K. Bauckhage, V. Uhlenwinkel (Eds.), Kolloquium des SFB 372, Vol. 4, Universität Bremen, 1999, pp. 21–44, ISBN 3-88722-440-X.

[3] H.R. Müller, Eigenschaften und Einsatzpotential sprühkompaktierter Kupferlegierungen, in: K. Bauckhage, V. Uhlenwinkel (Eds.), Kolloquium des SFB 372, Vol. 1, Universität Bremen, 1996, pp. 33–56, ISBN 3-88722-363-2.

[4] O. Meyer, U. Fritsching, K. Bauckhage, Numerical investigation of alternative process conditions for influencing the thermal history of spray deposited billets, in: Conference on Spray Deposition and Melt Atomization, Vol. 2, Bremen, Germany, June 26–28, 2000, pp. 771–788.

[5] K. Jambunathan, E. Lai, M. Moss, B. Button, A review of heat transfer data for single circular jet impingement, Internat. J. Heat Fluid Flow 13 (2) (1992) 106–115.

[6] F. Gori, L. Bossi, On the cooling effect of an air jet along the surface of a cylinder, Internat. Comm. Heat Mass Transfer 5 (2000) 667–676.

[7] C. McDaniel, B. Webb, Slot jet impingement heat transfer from circular cylinders, Internat. J. Heat Mass Transfer 43 (2000) 1975–1985.

[8] T. Pekdemir, T. Davies, Mass transfer from stationary circular cylinders in a submerged slot jet of air, Internat. J. Heat Mass Transfer 41 (15) (1998) 2361–2370.

[9] C. Gau, C. Chung, Surface curvature effect on slot-air-jet impingement cooling flow and heat transfer process, Trans. ASME J. Heat Transfer 113 (1991) 858–864.

[10] E. Sparrow, C. Altemani, A. Chaboki, Jet-impingement heat transfer for a circular jet impinging in crossflow on a cylinder, Trans. ASME J. Heat Transfer 106 (1984) 570–577.

[11] A. Tawfek, Heat transfer due to a round jet impinging normal to a circular cylinder, Heat Mass Transfer 35 (1999) 327–333.

[12] H.D. Baehr, K. Stephan, Wärme- und Stoffübertragung, 2. Auflage, Springer, Berlin, 1996.

[13] Verein Deutscher Ingenieure VDI, VDI-Wärmeatlas, 8. Auflage, Springer, Berlin, 1997.

[14] C. Kramer, Die Kompaktierungsrate beim Sprühkompaktieren von gaußförmigen Depositen, Dissertation, Universität Bremen, 1997.

[15] S.C. Koria, K.W. Lange, An experimental study on the behaviour of an underexpanded supersonic gas jet, Arch. Eisenhüttenwesen 55 (9) (1984) 427–432.